Experimental Study of Rotor Performance in Deep Ground Effect with Application to a Human-Powered Helicopter

Joseph Schmaus[1] Benjamin Berry[2] William Gross[3] Panagiotis Koliais[4]

Alfred Gessow Rotorcraft Center
Department of Aerospace Engineering
University of Maryland, College Park, MD 20742

ABSTRACT

A study of ground effect performance is presented with specific applications to *Gamera*, a human powered helicopter. This parametric study quantifies ground effect for four different rotors: a baseline (no twist/no taper), negative twist/no taper, positive twist/no taper, and taper/no twist. Data for these four rotors are presented in power polars and as global performance improvements. A brief study is made of how to apply these measurements to predictions of performance in ground effect. Comparisons between the individual rotors are then used to inform design decisions for helicopters being optimized for ground effect, specifically *Gamera*. Performance measurements from a *Gamera* rotor in deep ground effect are presented.

NOTATION

A	Rotor disc area, ft^2
$c(r)$	Chord distribution, ft
c_{75}	Chord at 75% radius, ft
c_{root}/c_{tip}	Taper ratio
C_P	Power Coefficient, $P/\rho A(\Omega R)^3$
C_T	Thrust Coefficient, $T/\rho A(\Omega R)^2$
k	Induced power factor
k_G	Ground effect induced power factor
R	Rotor radius, ft
Re_{tip}	Tip Reynolds number
z	Height above the ground, ft
z/R	Height to radius ratio
λ_i	Induce inflow
Ω	Rotor speed, rad/s
ρ	Air density, slug/ft^3
σ	Thrust weighted solidity, $(3N_b/\pi R)\int c(r)r^2dr$
θ_o	Collective pitch
θ_{tw}	Tip twist relative to the root

Abbreviations

IGE	In ground effect
OGE	Out of ground effect

[1] Graduate Research Assistant. **jschmaus@umd.edu**
[2] Graduate Research Assistant. **benberry@umd.edu**
[3] Undergraduate Researcher. **will.f.gross@gmail.com**
[4] Graduate Research Assistant. **pkoliais@gmail.com**

Presented at the American Helicopter Society 68th Annual Forum, Fort Worth, Texas, May 1-3, 2012.

INTRODUCTION

Team *Gamera* from the Alfred Gessow Rotorcraft Center at the University of Maryland designed and flew a human powered helicopter, named *Gamera I*, in the summer of 2011. Judy Wexler, a graduate student at UMD, flew the vehicle a total of 6 times. Her longest flight, lasting 11.4 seconds, holds the Fédération Aéronautique Internationale (FAI) world record for hovering duration of a human powered helicopter in the general and feminine categories. Figure 1 shows the record holding flight. The ultimate test for a human powered helicopter is the Sikorsky Prize (Ref. 1) established in 1980, which requires a hovering duration of 60 seconds while momentarily reaching an altitude of 3 meters (9.8 ft). Data from rotor tests, analytic rotor models, and human power testing (Ref. 2) combined with flight test experience, suggested that even with a pilot of Judy's high level of fitness, *Gamera I* had a maximum flight time of only 10-20 seconds. This motivated the design of *Gamera II*,

Figure 1. *Gamera I*, a human powered helicopter, in flight at the Reckord Armory on the University of Maryland Campus

focusing on minimizing the total weight of the vehicle and designing a more efficient rotor (Ref. 3). As part of this effort, a detailed study of ground effect performance on a sub-scale rotor was undertaken by the team. Based on the sub-scale experimental results a design was selected for *Gamera II*'s rotor and this rotor has been tested across a range of heights.

Ground effect is a term that is used to describe the changes in performance that both rotorcraft and fixed wing aircraft experience as they approach the ground. In rotorcraft it is used to allow an overloaded helicopter to transition to forward flight for takeoff and to provide part of the air cushion an autorotating helicopter relies on for a safe landing. For this reason, ground effect is often viewed as an increase in thrust for a constant power. A key parameter when looking at ground effect is the height above the ground, traditionally represented as a non dimensional ratio with the rotor radius (z/R). In most helicopters the rotor is placed above the fuselage, creating a practical *minimum z/R* value of 0.5. Rotors on human powered helicopters have radii of 20-50 ft and are placed as close to the ground as possible to maximize the impact of ground effect. This limits the *maximum z/R* of a human powered helicopter less than 0.5. The region with $z/R < 0.5$ was labeled deep ground effect in these experiments to differentiate it from the higher heights and more marginal improvements seen by a traditional helicopter. Human Powered helicopters have other unique features affecting the way ground effect is measured. Figure 2 shows how the constant power output a human can sustain is a strong function of the duration of the activity. The combined weight of the pilot and aircraft are constant suggesting that it is more natural to look at ground effect as a savings in power at a constant thrust.

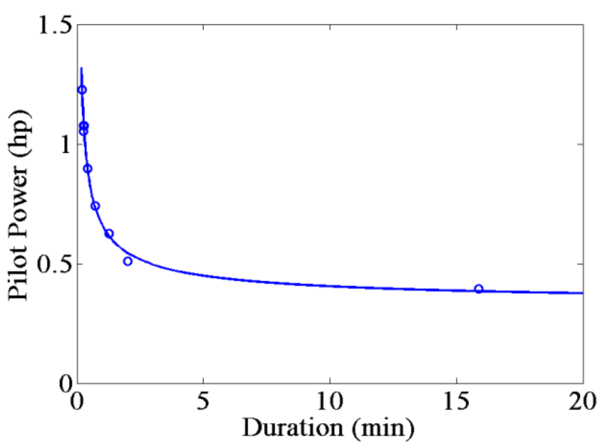

Figure 2. Constant human power shown against the duration that power can be maintained, from Kyle Gluesenkamp, *Gamera* test pilot (Ref. 3)

Many experiments have been performed to measure the impact of ground effect on the performance of a hovering rotor (Ref. 4-11). Of particular interest to this study is the early work of Knight and Hefner (Ref. 4) who studied the impact of number of blades on untwisted rotors to a z/R of 0.25. Fradenburgh (Ref. 7) measured rotor performance as low as a z/R of 0.1 and performed detailed studies of the flow field beneath the rotor. He observed that the rotor wake did not contract in the usual way, but rather the tip vortices moved radially out from the rotor as they approached the ground and there was an area of dead air, or even up wash, near the root. Fradenburgh subsequently observed (Ref. 9) that for a rotor with -8° twist and a rotor with -16°, the more highly twisted rotor performed better out of ground effect but worse in ground effect. Koo and Oka (Ref. 8) performed detailed flow studies of a rotor hovering down to a z/R of 0.125 and showed that the inflow was on average reduced. They concluded that "when the blade pitch angle is big, stalling sometimes occurs when the rotor approaches the ground."

Several global models have been suggested to predict ground effect performance with application to helicopter design (Ref 12-14). Prescribed wake models have provided some accuracy (Ref. 15) in predicting rotor flow physics. Free wake models (Ref. 16) and CFD studies (Ref. 17) have also been performed and show good correlation with data but these methods are not yet robust enough to provide guidance for design decisions.

EXPERIMENTAL SETUP

Rotor Blades

For this experiment, three fiberglass two-bladed rotors were used. Table 1 summarizes the sets of blades (Figure 3) including: no twist/no taper, twist/no taper, and taper/no twist. The airfoil selected was NACA 0012 because of its traditional use as a baseline airfoil. The symmetric nature of the airfoil allowed the twisted blades to be used to determine the performance of both negative twist and positive twist in ground effect. Negative twist rate means the tip of the blade has a lower pitch angle than the root and positive twist has a higher pitch angle at the tip. This doubling of the uses for the twisted blade brought the total rotor configurations studied to four. Each configuration was tested at 117 RPM (for a tip speed of 55 ft/s) across collective pitch values varying from 0° to 16°. Root cutouts extended up to 13% radius and the blade grips extended to 18% radius to rigidly hold the rotor. Resulting experiments spanned disk loadings up to .15 lb/ft^2 and C_T/σ of 0.15.

Table 1. Characteristics of the three sets of blades used in testing

	Baseline	Twisted	Tapered
Airfoil	NACA0012	NACA0012	NACA0012
Radius (ft)	4.5	4.5	4.5
c_{75} (ft)	0.86	0.83	0.84
c_{root}/c_{tip}	1:1	1:1	2:1
θ_{tw} (°/R)	0	-7.5	0
σ	0.122	0.117	0.119
Re_{tip}	280,000	270,000	250,000

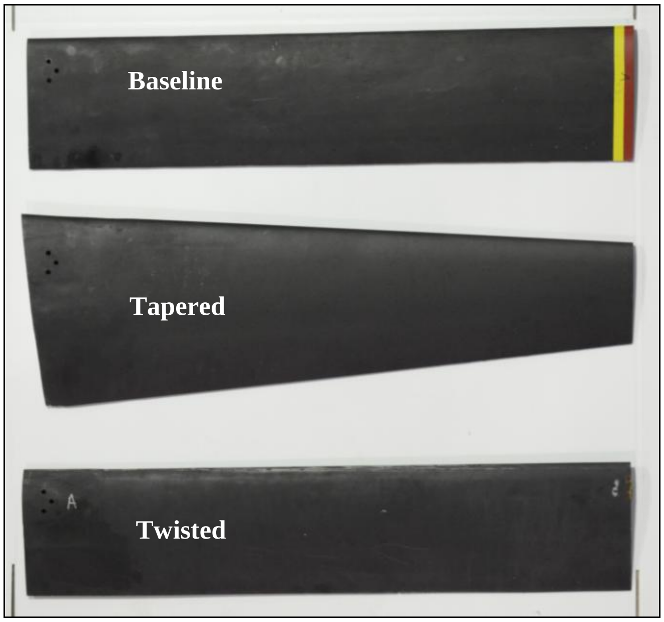

Figure 3. The three blade geometries used in this study, from top to bottom; baseline, tapered, and twisted

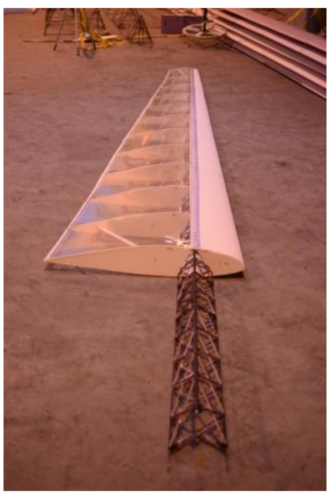

Figure 4. A *Gamera II* rotor blade

All rotor blades used in testing were manufactured using the same technique. A Computer Numerical Controlled (CNC) hot-wire cutter was used to cut extruded polystyrene foam cores. Low rotational speeds (117 RPM) and low loads (thrust was less than 10 lb) meant that a traditional spar was not required. Instead the root was reinforced with a solid 4 in. x 4 in. block of pine inserted in the foam at the root to connect with the hub. It was then sanded to match the contour of the airfoil and secured to the foam using vacuum cured [0 90] carbon fiber prepreg. The remaining portion of the blade was then covered with a fiberglass sleeve and epoxy composite, also vacuum cured. Finishing included filling in voids with extra epoxy and then sanding the surface smooth with a focus on the leading edge. Finally, the blade tips and trailing edges were trimmed to the appropriate size and the blade was painted. One of each pair of blades is shown in Figure 3. Both the twist and taper were distributed about the quarter chord of the blade.

As far as possible, the rotor parameters were selected to represent a typical human powered rotor system. For comparison, the *Gamera I* rotor (Ref. 2) had a 21.3 ft radius and a 3.3 ft chord with no twist or taper and used an Eppler 387 airfoil. The *Gamera II* (Ref. 3) rotor blade is shown in Figure 4. The rotor radius was 21.3 ft and the chord at 75% radius was 1.8 ft with a taper ratio of 3:1. The airfoil was the Selig S8037 and no twist was applied. The operational speed was 17 to 20 RPM yielding tip speeds of 40 ft/s, corresponding to Reynolds numbers of 750,000. The total weight of the vehicle was around 200 lb for each configuration and shared across 4 rotors, so that each rotor carried 50 lb. This corresponds to a disk loading of 0.04 lb/ft^2 and a C_T of 0.01. Despite the variation in Reynolds number, the comparable tip speed and disk loading was expected to be valuable in predicting performance of the full scale rotor based on this experimental study.

Ground Effect Test Rig

The Ground Effect Test Rig (GETR) was constructed by Team *Gamera* to help evaluate the impact of ground effect on the various rotor geometries. The experiment was designed and built around a rolling gantry crane as shown in Figure 5. The crane served as both the support structure for

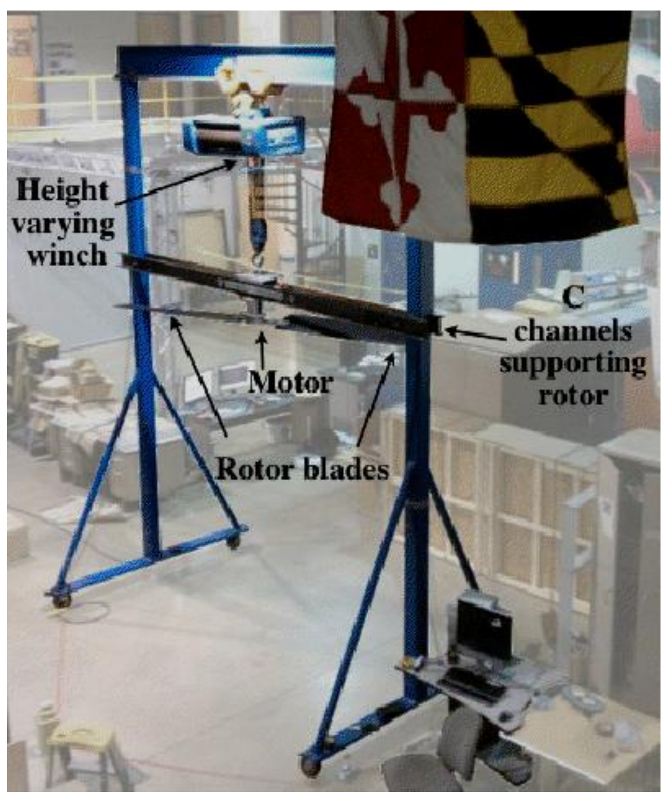

Figure 5. GETR with baseline blades attached

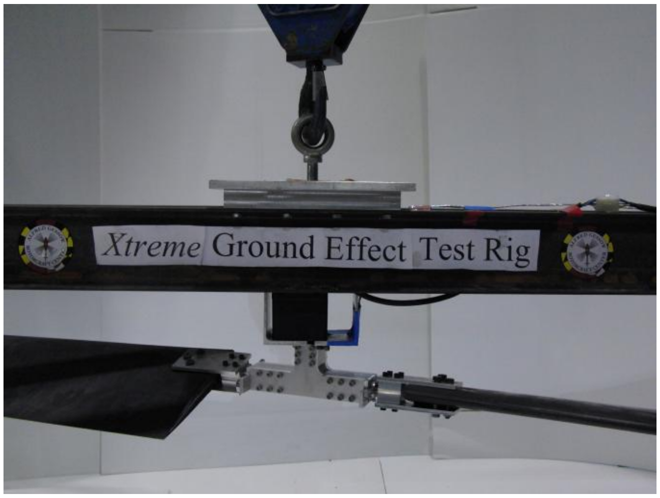

Figure 6. GETR rotor hub with the twisted blades attached. The motor gearbox can be seen below the C-beams and above the aluminum hub

the hover stand and as the winching system for the adjustment of rotor height above the ground. The motor and sensor equipment was mounted between two parallel C-channel beams that were loosened for vertical movement, but provided rigid attachment to the frame during the tests. A plate was used to connect the C-beams and act as a base for the testing apparatus. The combined load/torque cell was mounted below the plate and the motor was mounted to the bottom of the load cell. Finally, the Hall effect sensor was placed between the motor face and the rotor hub. A more detailed view of this assembly is shown in Figure 6.

An Oriental Motors AXU series brushless motor and speed control with an 18:1 gear ratio was used to drive the system. The motor was run in both the clockwise and counterclockwise directions with equal effectiveness. A Cooper instruments LXT-920 combined 200 in-lb torque cell and 200 lb load cell was used to measure the resultant loads. Measured torques were on the order of 40 in-lb while applied loads were less than 25 lbs. The linearity of both devices was 0.2% and the repeatability was 0.05% which was expected to be sufficient for this application. Two neodymium magnets were placed on the hub at the roots of the blade and a Hall effect switch was attached to the motor to provide a 2/rev pulse for measuring RPM.

All data was read in by a National Instruments SCC-2345 and USB-6251 data acquisition (DAQ) system. The torque and thrust were read using SCC-SG24 modules and RPM was read with an SCC-FT01. A LabVIEW program was written to provide real-time representation of the data to the operator while recording it in parallel for detailed post processing. Ambient temperature and pressure were entered manually into the LabVIEW system and recorded in the relevant data file for future use. Speed was controlled manually by the operator monitoring the RPM output in the LabVIEW program.

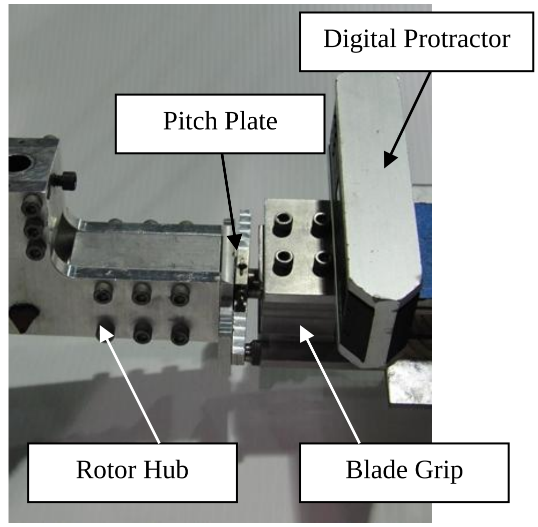

Figure 7. Close up of the GETR rotor hub

The rotor hub (Figure 7), consisted of a central hub that mounted on the motor shaft, pitch plates that could pitch relative to the hub, and blade grips that attached to the pitch plates. Preset collective pitch angle allowed for ± 16° pitch by steps of 2°. The blades were securely held in the blade grips by three bolts with the quarter chord at the pitch axis of the blade. The blade attachment to the pitch plate was maintained by a pair of set screws so that each blade's pitch could be adjusted during trim.

Full Scale Test Stand

The full scale test stand, shown in Figure 8, consisted of a 0.5 hp DC motor connected to the rotor shaft using a chain system with an effective gear ratio of 78:1. The shaft was instrumented with strain gages for measuring torque and had eight magnets distributed around the shaft read by a Hall effect switch for RPM. Four load cells placed at the corners of the test stand were used to calculate the steady thrust and fixed-frame hub moments. All data was collected using the same DAQ system used on GETR.

Figure 8. Full scale test stand at ground level with a *Gamera I* rotor (above) and raised to a height of 10 feet with *Gamera II* blades attached (below)

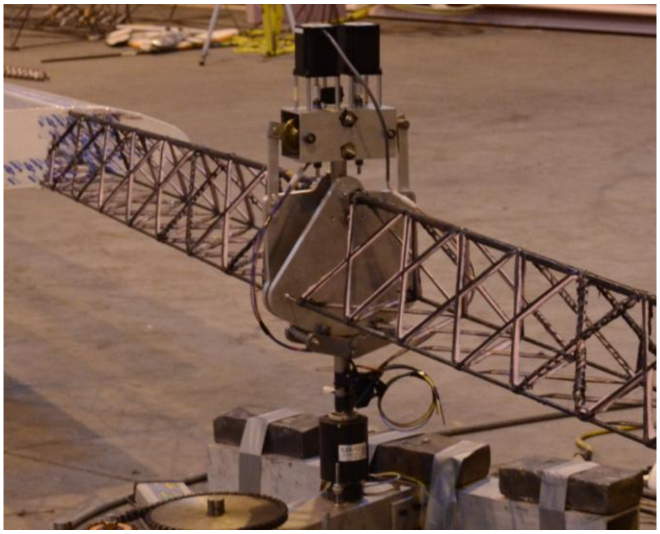

Figure 9. Motorized hub used to provide individual control of the rotor blades on the full scale test stand, with *Gamera II* rotor attached

The hub (Figure 9) consisted of two pitch plates that rigidly attached to the three tubes used in each blade spar. The pitch plates were mounted on a series of bearings and connected to separate stepper motors. Each plate had an accelerometer attached that measured the pitch angle with respect to gravity. This allowed for independent rotating frame control of the rotor blades.

The lowest height was performed with the test stand placed on the ground. For the height sweep the test stand was mounded on a short scissor lift (Figure 8). It was securely strapped to the floor of the scissor lift with the rails removed.

METHOD

For each of the 4 rotors that were studied, the blades were first mounted on the rotor hub. Figure 7 shows a digital protractor that was used to set each blade to 0° pitch angle using both the pitch set screw and the thumb screw. Recognizing that a zero angle of attack of the blade grips may not be the angle that actually produces minimum power, a collective sweep was performed to trim the rotor for minimum power (Figure 10). One blade was set to a pitch angle of 2 degrees while the second was kept at 0 degrees. The pitch angle of the first was swept until a minimum point on a torque versus angle of attack curve was established. This angle was then fixed as 0 on the pitch plate using the set screw. The same procedure was then repeated with the second blade.

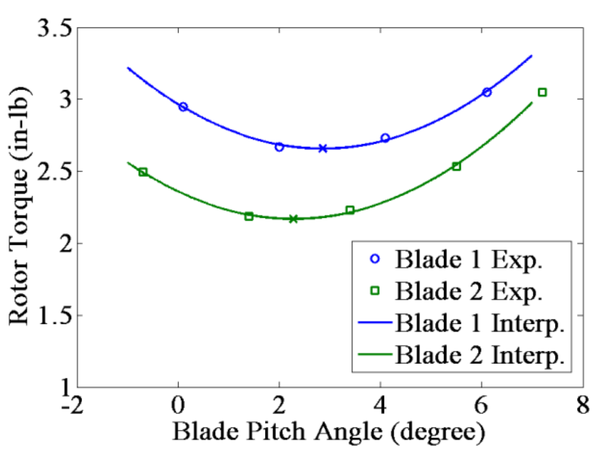

Figure 10. Illustration of how individual blade angles are swept for minimum power to identify trim angles

In this experiment, *z/R* heights of 0.1, 0.2, 0.5, 1.0, 1.75, and 2.0 were explored for each of the four rotor geometries. For each height, the C-beams were loosened and the crane was used to raise the platform. The quarter chord of the rotor was used to measure the height of the rotor. For high *z/R* values this was not critical, but at lower heights the trailing edge of the rotor came very close to the ground as the height approach the length of the chord and the choice of reference became significant. Before securing the platform in place, the C-beams were leveled with a digital protractor.

At the beginning of each height the rotor was always set to an initial azimuth angle for consistency of zeros. The pitch of the blades, the height above ground, and the target rotor RPM were entered in the LabVIEW program along with the ambient pressure and temperature. All rotor tests presented in this paper occurred at 117 RPM. Load cell and torque cell zeros were recorded in LabVIEW by taking data for 20 seconds at 0 RPM. The motor was then spun up to the desired RPM and 20 seconds of data was recorded at this RPM. The rotor was then stopped and another zero was taken. This process was repeated until three data points at the operational RPM were taken. The blades were then returned to the initial azimuth angle and a final zero was taken. A preliminary check of the data was made by plotting both load and torque versus RPM. If the variation was within appropriate tolerances, the rotor test proceeded. This procedure was completed for all collectives from 0° to 16° by steps of 2°, completing a full range of collective sweeps at a particular *z/R*. This entire process was completed at each of the *z/R* values. Once a height sweep for a given rotor was complete, a new set of blades was placed on GETR and tested.

Data Reduction

The data was examined two different ways. First, experimental points were examined directly to provide insight into how the performance shifted with collective angle. Second, specific C_T/σ or C_P/σ values were interpolated between the experimental points and used to generate traditional representations of ground effect's impact on performance.

Each test condition (defined by rotor configuration, *z/R*, and θ_o) consisted of at least three data points and several zero values. The median of the zeros was used for all tests at that condition to limit the impact of data drift and remove the impact of slight variations in test setup between configurations. Temperature and pressure were used to calculate the air density value. C_P and C_T values were calculated as described in the notation section using this local density value and the RPM recorded by the Hall effect switch for each test. The data was further divided by the thrust weighted solidity, σ, to remove the impact of blade area, particularly when comparing tapered to untapered blades.

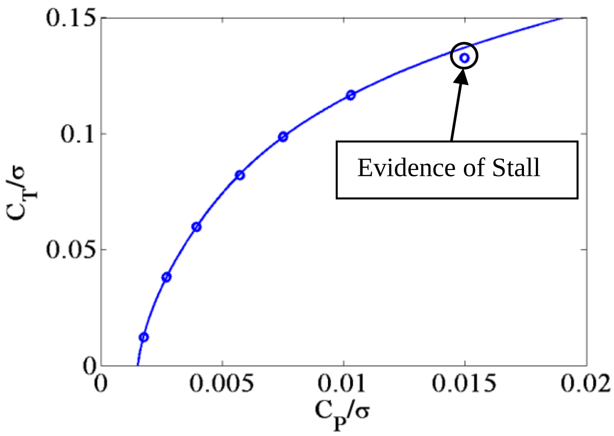

Figure 11. Collective sweep of the baseline rotor at a *z/R* of 0.20 with an interpolated best fit line

At each height the data in the sweep were interpolated by a polynomial, an example of which is shown in Figure 11. In some cases a polynomial could not properly capture high powers associated with high collectives in deep ground effect without adding extra oscillations or poorly representing the data. These cases correlate with sharp power increases that are discussed later and are likely correlated with stall. Therefore these points were not included in the interpolations. This is illustrated by the point with a C_T/σ value of 0.13 in Figure 11.

Full Scale Tests

For the full scale tests heights with a *z/R* of 0.30, 0.39, 0.54, 0.63, 0.71, and 0.86 were examined. While these do not come close to the OGE value, they were chosen because they cover the range of heights *Gamera II* would experience completing the Sikorsky prize. At each height the scissor lift was secured and a zero was taken with the rotors stationary. Then rotors were spun up to 20 RPM with the pitch set low and the rotors were balanced. The individual blade control and moment data from the four load cells were used to ensure that the net lift was shared evenly between the two rotor blades for optimal performance and safety of the rig and personnel. With the rotor still spinning the collective was increased and a thrust sweep was taken in a single test. Ambient temperature and pressure were recorded in the LabVIEW program and the resulting data was analyzed in a similar way to the GETR tests.

RESULTS

Baseline

The first GETR experiments were performed with the no twist/no taper rotor. These blades provided both a useful comparison for *Gamera I*, which had the same characteristics, and could act as a baseline against which to compare the other rotors. All the data collected for this set of blades are summarized in Figure 12. Note that the power savings is quite large at the highest C_T/σ values. As thrust is reduced the power curves for all heights approach a constant value. This agrees well with the theory that ground effect is primarily an effect on the induced inflow velocity and does not significantly impact profile power. While there is a large difference in power between *z/R* of 0.1 and 0.2 the data for *z/R* of 1.75 and 2.0 lay almost on top of each other. This is an encouraging sign that the data at *z/R* of 2.0 is close to representing the out of ground effect values.

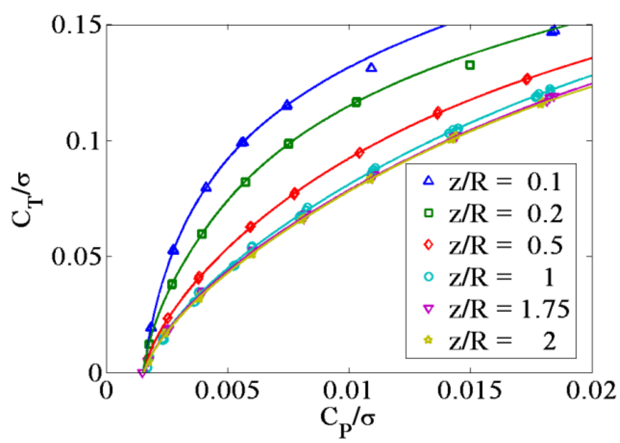

Figure 12. Data points from baseline (untwisted blade tests) presented with interpolated trend lines

It can be instructive to look at constant collective values. At constant collective, the rotor behaves the same across the range of heights and only the flow field changes, making these curves the most likely to highlight the fundamental physics of the problem. Figure 13 presents the power for a selected subset of collectives across the full range of heights. At the highest collective (θ_o = 16°) the power noticeably increases at low heights. At lower collectives the changes in power are significantly smaller. This sharp increase in power for the highest collective suggests that the rotor angles of attack are high enough to begin showing signs of stall. Figure 14 shows rotor thrust for these same height and collective points. It is possible to see how thrust gradually increases at lower *z/R* values. If thrust is modeled with Equation (1),

$$\frac{C_T}{\sigma}_{IGE} = \frac{C_T}{\sigma}_{OGE} + \Delta\frac{C_T}{\sigma} \tag{1}$$

the relevant $\Delta C_T/\sigma$ values for collectives of 4° to 16°are shown in Figure 15. It is interesting to note that while

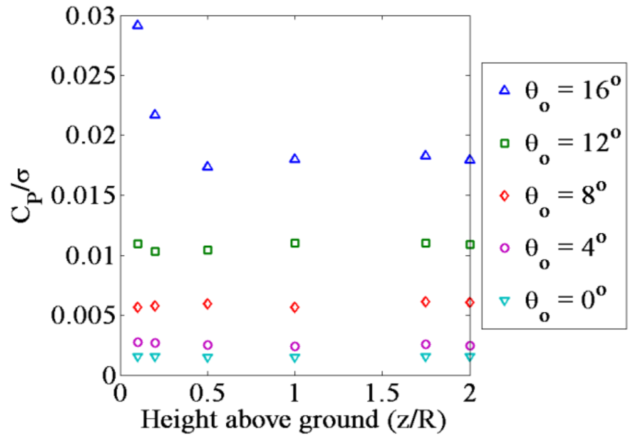

Figure 13. A limited selection of power at constant collective for the untwisted baseline rotor

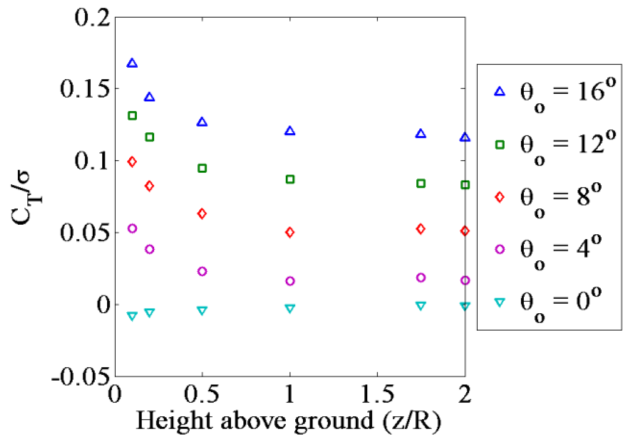

Figure 14. A limited selection of thrust at constant collective for the untwisted baseline rotor

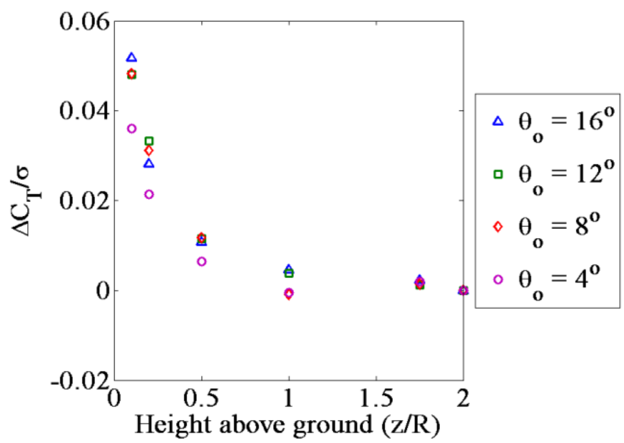

Figure 15. $\Delta C_T/\sigma$ values at constant collectives for the untwisted rotor

C_T/σ_{OGE} is proportional to the collective, $\Delta C_T/\sigma$ shows a much a much weaker correlation.

Presenting performance data on a power polar or from constant collective curves provides an overview of how the rotor behaves in ground effect. However, design insight requires a more direct view of how ground effect impacts performance. It is therefore useful to present data as either constant power or constant thrust slices through a power polar like Figure 12.

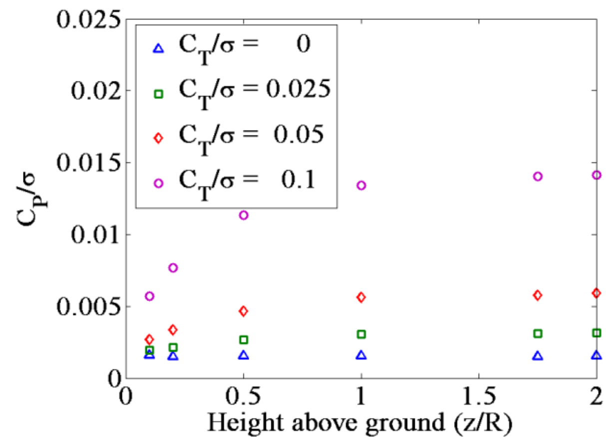

Figure 16. Constant thrust curves for the untwisted baseline rotor

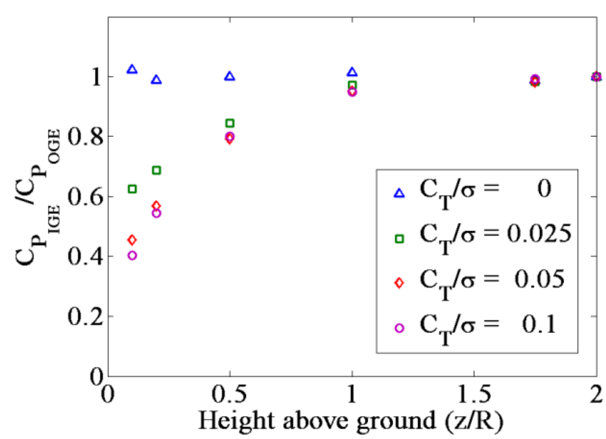

Figure 17. Normalized constant thrust curves for the untwisted baseline rotor

Power variation with constant thrust is shown in Figure 16. While it can be seen that the required power decreases as the rotor approaches the ground, the extent of this change across various thrust levels is not obvious. To resolve this, the data is normalized by the *z/R* = 2.0 values, which are assumed to approximate OGE power. This highlights the effective power savings for various thrust levels, shown in Figure 17. The power savings is comparable between the high C_T/σ values of 0.05 and 0.1. Below this range the power savings begins to decrease significantly. The small variation in power at zero thrust can be attributed to measurement error.

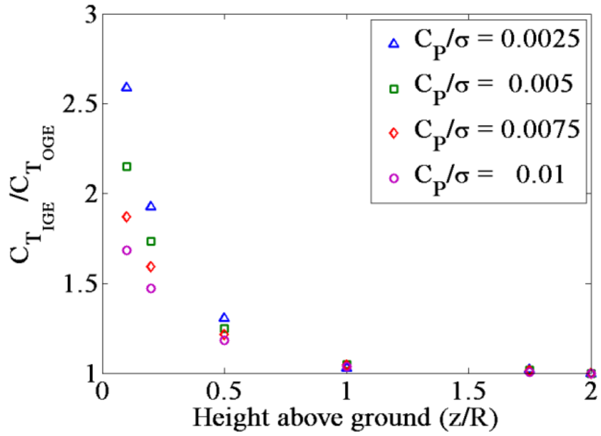

Figure 18. Normalized constant power curves for the untwisted baseline rotor

Thrust variation with constant power is a second way to look at this data. The thrust ratios shown in Figure 18 were found to decrease with higher levels of power. This is a result of the fact that $\Delta C_T/\sigma$ tends to be consistent between powers, whereas C_T/σ_{OGE} increases. This is the traditional method for representing ground effect improvements, but here the thrust ratios show a strong dependency on C_P/σ, suggesting that any trends identified from this data would have to be a function of both height and power level.

Parametric Study

Taper is an essential part of the ideal hovering rotor and has been shown in experiments to improve performance. While this has been shown time and again to be true out of ground effect, there is no previously well established study that explores the effect of taper in comparison to untapered rotors when in ground effect. Figure 19 shows the power polar for the tapered rotor used in this experiment. At the *z/R* values of 1.75 and 2.0, the curves lie almost on top of each other, suggesting that these are close to being the OGE values. Also, as the thrust level decreases the curves collectively have a uniform power at the lowest thrust corresponding to the profile power.

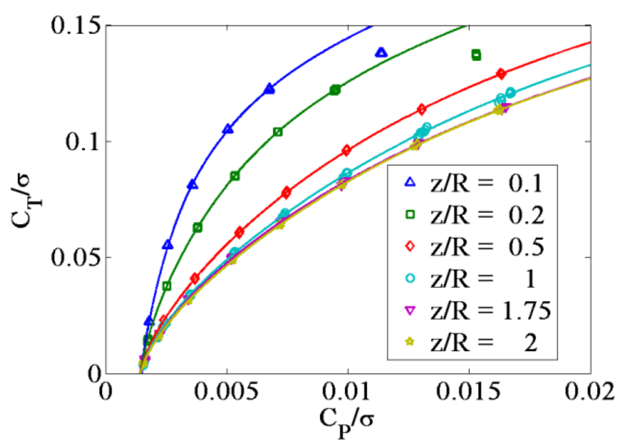

Figure 19. Data from 2:1 taper rotor presented with interpolated trend lines

Negative twist is another common blade design parameter that improves rotor efficiency by reducing the induced inflow at the tip of the blade. Because twist modifies the inflow, it may not be intuitive how it impacts rotor performance in ground effect. The negatively twisted rotor appears to show similar characteristics to the baseline and tapered rotor, but Figure 20 shows some noticeable differences. First, at *z/R* of 1.0 the performance is very close to the higher *z/R* values of 1.75 and 2.0. This is interesting because it suggests that for this twisted rotor ground effect benefits end at a much lower height. Also, the power is generally higher for every thrust.

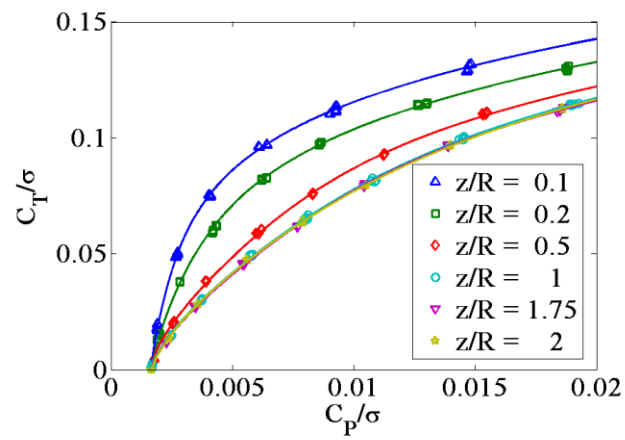

Figure 20. Data from -7.5° twist rotor presented with interpolated trend lines

The positively twisted rotor (Figure 21) has unique performance as well. It has the largest separation between performance at *z/R* values of 1.75 and 2.0, suggesting that

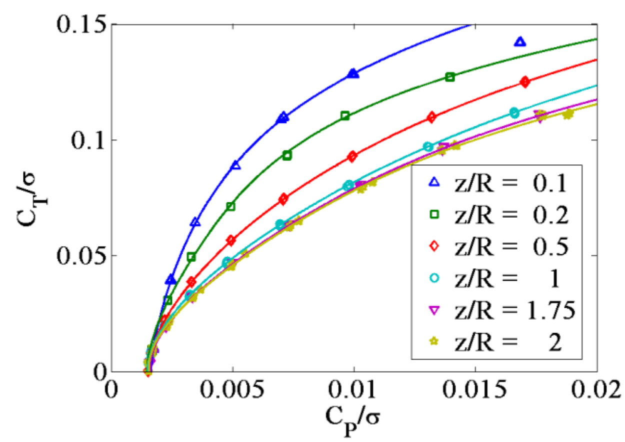

Figure 21. Data from +7.5° twist rotor presented with interpolated trend lines

the rotor may not yet be all the way out of ground effect at z/R = 2.0. The curves are spaced farther apart from each other than the negatively twisted case, indicating that positive twist has a greater impact from ground effect. The performance for each height is similar to the other heights up to a C_T/σ of 0.015 suggesting some unknown phenomenon caused by the positive twist at low thrust and low power.

When the thrust ratios for all four rotor configurations are placed on one plot (Figure 22), they can be compared to one another. The tapered rotor is clearly the most efficient rotor in this study, at the lowest z/R, although this advantage over the baseline and negatively twisted rotor has diminished by a z/R of only 0.2. The positively twisted blades perform the worst in deep ground effect, but this penalty is diminished by a z/R of 0.5. Because these curves are taken at such a low power (C_P/σ = 0.005) it is possible the positive twist values are being distorted by the behavior of positive twist at low thrust and power.

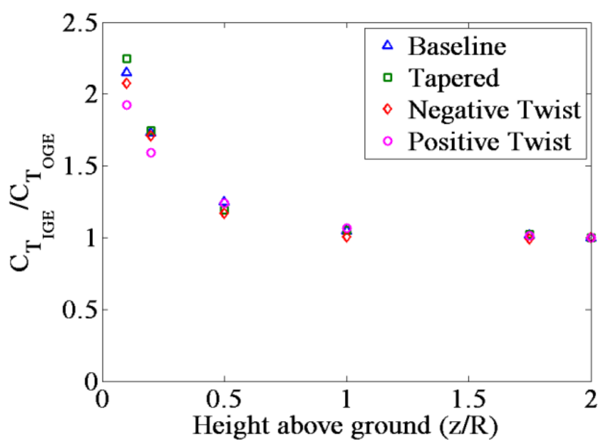

Figure 22. Comparison of the thrust ratios for C_P/σ = 0.005 across the 4 different configurations

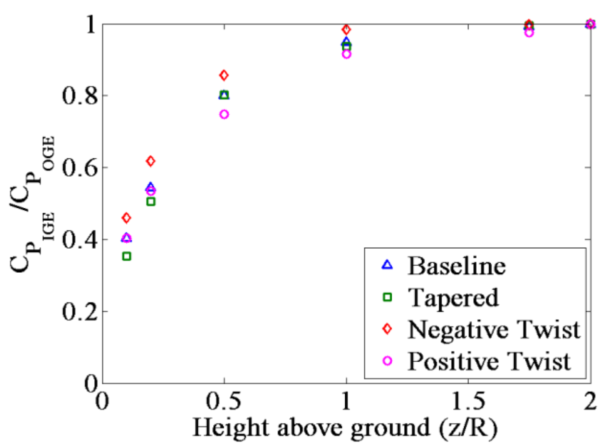

Figure 23. Comparison of the power ratios for C_T/σ = 0.1 across the four different configurations

Power ratios are more useful when comparing various configurations for a human powered helicopter and are shown collated for C_T/σ = 0.1 (Figure 23). It is again clear that the tapered blades have the best performance in deep ground effect followed by the baseline and positive twist. Finally the negatively twisted blades have the worst performance. This trend is fundamentally different from the thrust ratio case where positive twist performs the worst. Across the high C_T/σ represented by the power ratios the issues with positive twist at low power discussed previously are less likely to be seen.

The baseline rotor has a 115% increase in thrust or a 60% reduction in power at a z/R of 0.1. For the same height, the tapered rotor has a 125% increase in thrust and a 65% reduction of power, a noticeable increase in performance. Positive twist provides an overall power savings comparable to the untwisted blades at 60%, and negative twist has the lowest power savings at only 54%.

Full Scale Tests

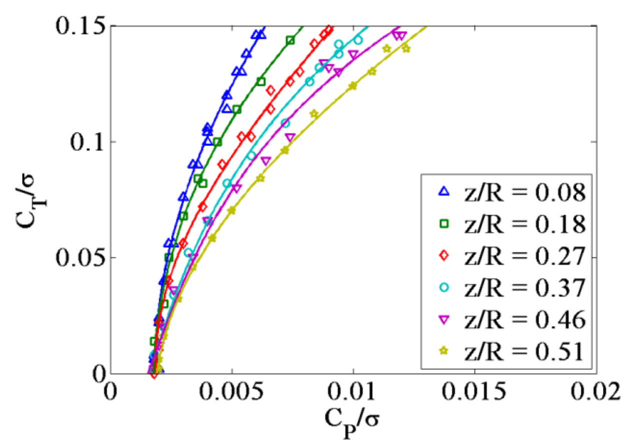

Figure 24. Data from full scale rotor tests of the *Gamera II* rotor presented with interpolated trend lines

Full scale rotor tests (Figure 24) show consistently improved performance over the subscale tests and this is likely due to the higher Reynolds number and an airfoil selected specifically for its performance at that Reynolds number. Because of the relatively soft and fragile skin, distortions of the airfoil occurred between the blade ribs from both bending related effects and variations in internal pressure distribution from centrifugal pumping. This phenomenon, noted in early cloth rotorcraft blades (Ref. 5, 18), were likely the cause for the scatter in the data, especially at z/R = 0.46. The performance curves at every height collapse to the same power at zero thrust, again suggesting that the profile power in this case is again independent of rotor height.

ANALYSIS

Ground effect is fundamentally an inflow related phenomenon. Because drag coefficients are somewhat insensitive to angle of attack, ground effect has a minimal impact on profile power until the rotor begins to experience large angles of attack approaching a stall condition. All the power polars for the configurations shown earlier demonstrate this through collapsing to a single power value for all the heights when thrust is zero. For the no thrust, case there is no induced inflow and therefore no mechanism by which ground effect can act.

This modification to inflow by which ground effect operates can be modeled by taking cues from constant collective curves. These are useful because the rotor has a constant geometry and only the flow field changes. It is interesting to see in these cases that the power does not change dramatically with height while the thrust does. At each height, every collective pitch (other than θ_o = 0°) showed similar $\Delta C_T/\sigma$ to the others, as shown in Figure 15. The expectation was that these $\Delta C_T/\sigma$ values would be proportional to induced inflow, and therefore thrust level. This unexpected result may provide some useful insight when developing future analytical or computational models.

Ground Effect Modeling

Non-dimensional ratios are useful in presenting ground effect performance improvements. Thrust ratios are useful because they follow the basic physics of the fixed pitch curves, represent the data in the way it is used in traditional helicopters, and isolate the impact of profile power. However, in deep ground effect, C_T/σ values exceed 0.13 (and therefore exhibit stall behavior in this data set) at extremely low powers. Power ratios illustrate ground effect behavior at a constant thrust across a large range of C_P/σ values, allowing the rotor to behave with a relatively constant angle of attack rather than constant θ_o.

The major caution when using power ratios is that they include profile power effects in the global ratio rather than isolating the impact on induced power. Therefore it is more appropriate to develop a k_G factor that only impacts the induced power as shown in Equation (2).

$$C_P = k_g k \lambda_i C_T + C_{P_o} \tag{2}$$

To arrive at this factor the profile power must be subtracted from individual power values before taking the power ratio. Fortunately, the power polars for each configuration show a unique profile power across all heights. The resulting k_G values are shown in Figure 25. A fourth order polynomial, while arbitrary, represents the baseline data quite well and is included as Equation (3).

$$k_G = -.157\left(\frac{z}{R}\right)^4 + 0.932\left(\frac{z}{R}\right)^3 \ldots \\ -2.068\left(\frac{z}{R}\right)^2 + 2.090\left(\frac{z}{R}\right) + .146 \tag{3}$$

Examining the k_G values reveals some interesting trends in the data. Noticeably, induced power reductions of over 70% are seen. However, the slope is quite steep in deep ground effect and by the time a *z/R* of 0.5 is reached, the power savings have been reduced to only 20%. Between *z/R* of 0.5 and 1.0 the trend begins to level off and above a *z/R* of 1.0 the induced power savings is less than 10% and the curve is almost linear.

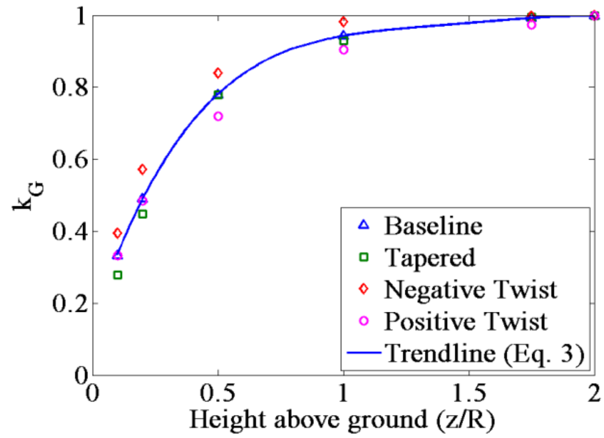

Figure 25. Induced power factors based on experimental data

Applications to Human Powered Helicopters

Ultimately, this study was performed to inform design decisions for a human powered helicopter. Both *Gamera I* and *Gamera II* have four large two-bladed rotors, requiring a total of eight rotor blades. Application of twist and taper add significant complexity in manufacturing and therefore need to be balanced against performance benefits. Figure 26 shows the total power which results when k_G values from Figure 25 are applied to the induced power calculated using classical BEMT out of ground effect.

Taper continues to be beneficial in ground effect. The out of ground effect rotor performance is improved by taper almost as much as it is by twist. In addition, taper sees an

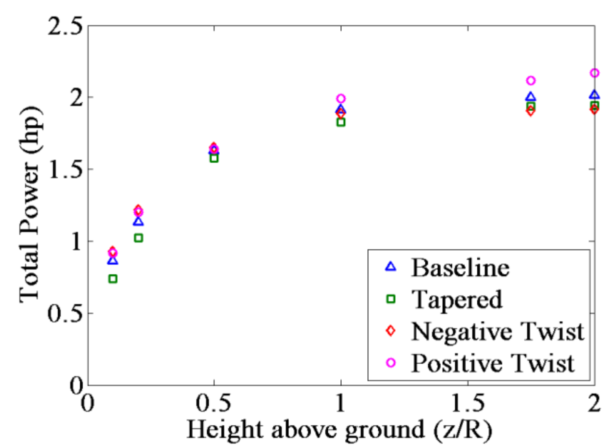

Figure 26. Notional application of ground effect methods to a human powered helicopter rotor

astounding 62% power savings in ground effect. Overall, adding taper should dramatically improve the performance of a human powered helicopter. A more detailed trade study is shown in Ref. 3 with much more attention paid to aerodynamic/structural interactions, total vehicle weight, and several other factors.

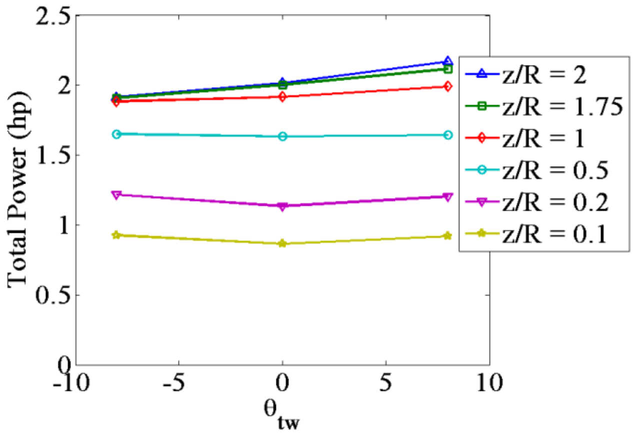

Figure 27. Power required at several heights plotted against twist rate

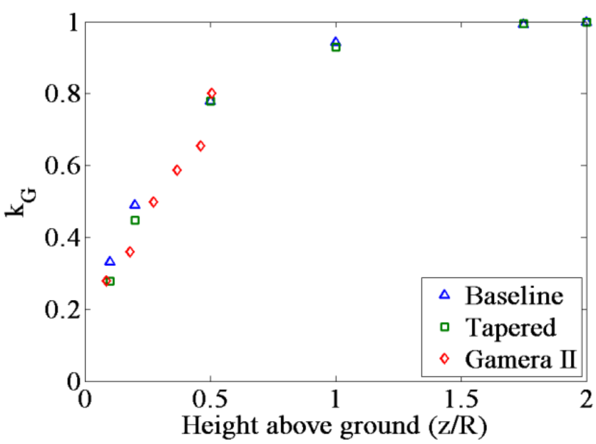

Figure 28. Estimated k_G value for baseline and tapered rotors compared with *Gamera II* rotor tests

Twist, on the other hand, does not show such a likely benefit. While negatively twisted blades reduce OGE power, in these experiments they were much less sensitive to ground effect than untwisted blades. Positive twist has a negative effect on OGE performance but at least it shows similar ground effect performance to the untwisted case. Figure 26 shows that for a notional human power helicopter, the same performance in deep ground effect is achieved for both positive and negative values of twist. An explanation for this is likely related to the benefits from twist, which come from flattening the inflow distribution. This is less beneficial in ground effect, where the natural inflow reduction performs this feat already. A possible explanation for the consistent behavior of the positively twisted rotor is that zero thrust, or minimum power, values for twisted rotors occur when the lift across the inboard and outboard sections of the rotor are equal and opposite. This implies that near the ground, the portion of the rotor thrusting up is seeing ground effect benefits, while the portion thrusting down is not,

The increased complexity in manufacture suggests that twist is not needed in the design of human powered helicopters. However, this study only focused on a limited set of twist values of -8°, 0°, and +8°. Figure 27 shows the power ratios at constant heights against varying twist rate. Clearly, the negatively twisted rotor performs better out of ground effect but this advantage is no longer true by *z/R* of 1.0. In contrast, the positively twisted rotor starts out the poorest and almost approaches the baseline rotor by the lowest height. This suggests that a more detailed sweep of twist might identify one or more optima at lower or higher twist rates that maintain an advantageous power across all heights.

Twisted rotors present a unique case. These rotors did not exhibit the expected behavior in ground effect; the negatively twisted rotor saw almost no benefit down to a *z/R* of 1.0 and the smallest benefit in deep ground effect.

The full scale rotor k_G can be evaluated using the same techniques (Figure 28). As with the subscale tests a clear profile power can be calculated from the curves and from that an induced power was calculated. For practical reasons the rotor was never tested at a height that approximates an out of ground effect condition. Therefore, a notional OGE induced power was used that assumed the IGE performance was the same between the *Gamera II* rotor and the tapered rotor experiments. With this assumption the induced power factor from the full scale tests show good agreement with the tapered rotor.

In addition to comparing with these models, the full scale tests also have relevance when evaluating the requirements of the Sikorsky Prize. The *z/R* value of 0.46 corresponds to the 3 meter height required by the Sikorsky Prize. At this height a vehicle weight of 200 lb results corresponds to a measured power of 1.3 hp. As can be seen in Figure 2, this is near the limit of human power available, even for very short durations.

CONCLUSIONS

A series of experiments were performed on four rotors with different twist and taper distribution across a range of *z/R* values. This data provides some guidance for design of a rotorcraft for flight in deep ground effect:

1) Taper provided benefits to OGE performance and had a lower estimated k_G than the baseline case. Therefore taper is likely to improve the performance.

2) Negative twist provided benefits to OGE performance, but saw much smaller IGE benefits than the baseline rotor, especially at high *z/R* values. The net result was

weaker than the baseline and should be applied only with great caution.

3) Positive twist showed penalties to OGE performance, and saw similar IGE benefits to the baseline. The net result was weaker than the baseline and positive twist is not indicated in or out of ground effect.

These data were important in the design and development of a full-scale human powered rotorcraft:

4) Tapered *Gamera II* rotor experiments showed good agreement with the performance levels expected from this data.

5) The 3 meter (9.8 ft) requirement of the Sikorsky Prize is attainable, but at the limit of human capability, even for a vehicle optimized for flight in deep ground effect.

Future work in ground effect optimization should focus on identifying why the thrust ratio is such a strong function of power level. More detailed studies of twist should be performed to identify whether there is an optimal linear twist rate or even a more complex twist distribution that optimizes IGE performance.

ACKNOWLEDGEMENTS

Support and advice for this study, and *Gamera* as a whole, has been provided by Dr. Inderjit Chopra, Dr. VT Nagaraj and Dr. Darryll Pines. The authors would also like to thank Tyler Fean, Mor Gilad, Garrett Hoppe, Christopher McDermott, Xing Wang, and Benjamin Woods for their experience and help in performing this study.

REFERENCES

[1] Sopher, R., “The AHS Igor Sikorsky Human Powered Helicopter Competition.” *Vertiflite*, 43(3), 1997, pp. 32-34.

[2] Schmaus, J., Berry, B., Bowen-Davies, G., Bush, B., Friedman, C., Gilad, M., Sridharan, A., Staruk, W., Woods, B. K. S., “Design and Development of *Gamera*: A Human Powered Helicopter from the University of Maryland,” *American Helicopter Society Future Vertical Lift Aircraft Design Conference*, San Francisco, CA, 2012.

[3] Berry, B., Bowen-Davies, G., Gluesenkamp, K., Kaler, Z., Schmaus, J., Staruk, W., Weiner, E., Woods, B. K. S., “Design Optimization of *Gamera II*: A Human Powered Helicopter,” *68th Annual Forum of the American Helicopter Society*, Fort Worth, Texas, 2012.

[4] Knight, M., and Hefner, R. A., “Analysis of Ground Effect on the Lifting Airscrew,” *NACA TN 835*, 1941.

[5] Gustafson, F. B., Gessow, A., “Flight Tests of the Sikorsky HNS-1 (ARMY YR-4B) Helicopter II – Hovering and Vertical-Flight Performance with the Original and an Alternate Set of Main-Rotor Blades,” *NACA MR L5D09a*, 1945.

[6] Zbrozek, J., “Ground Effect on the Lifting Rotor,” British ARC R&M 2347, 1947.

[7] Fradenburgh, E A, “The Helicopter and the Ground Effect Machine,” *Symposium on Ground Effect Phenomena*, Princeton University, NJ, 1959.

[8] Koo, J., Oka, T., “Experimental Study on the Ground Effect of a Model Helicopter Rotor in Hovering,” *NASA TT F-12,938*, Translation of NAL-TR-113, Tokyo, 1966.

[9] Fradenburgh, E A, “Aerodynamic Factors Influencing Overall Hover Performance,” *AGARD-CP-111*, 1972.

[10] Rossow, V. J., “Effect of Ground and/or Ceiling planes on Thrust of Rotors in Hover,” *NASA-TM-86754*, 1985.

[11] Lee, T E, Leishman, J G, Ramasamy, M, “Fluid Dynamics of Interacting Blade Tip Vortices with a Ground Plane,” *64th Annual Forum of the American Helicopter Society*, Montréal, Canada, 2008.

[12] Johnson, W., *Helicopter Theory*, Princeton University Press, Princeton, NJ, 1980, pp. 122-124.

[13] Stepniewski, W. Z., Keys, C. N., *Rotary-Wing Aerodynamics*, Dover Publications, New York, NY, 1984, Part II, Chapter 2.

[14] Leishman, J. G., *Principles of Helicopter Aerodynamics*, Cambridge University Press, New York, NY, 2006.

[15] Gilad, M., Chopra, I., Rand, O., “Performance Evaluation of a Flexible Rotor in Extreme Ground Effect,” *37th European Rotorcraft Forum*, Milan, Italy, 2011.

[16] Griffiths, D. A., Ananthan, S., Leishman, J. G., “Predictions of Rotor Performance in Ground Effect Using a Free-Vortex Wake Model,” *58th Annual Forum of the American Helicopter Society*, Montréal, Canada, 2002.

[17] Lakshminarayan, V. K., Kalra, T. S., Baeder, J. D., “CFD Validation of Micro Hovering Rotor in Ground Effect,” *66th Annual Forum of the American Helicopter Society*, Phoenix, AZ, 2010.

[18] Tetervin, N., “Airfoil Section Data from Tests of 10 Practical-Construction Sections of Helicopter rotor Blades Submitted by the Sikorsky Aircraft Division,” *NACA MR*, 1944.